Journal of Mining and Environment (JME) Vol. 15, No. 4, 2024, 1539-1562

Shahrood University of Technology

Journal of Mining and Environment (JME)

Journal homepage: www.jme.shahroodut.ac.ir

Iranian Society of Mining Engineering (IRSME)

Determination of the caving zone height using numerical and physical modeling based on the undercutting method, joint dip, and spacing

Behnam Alipenhani[1], Mehran jalilian[1], Abbas Majdi[1*], Hassan Bakhshandeh Amnieh[1] and Mohammad Hossein Khosravi[2]

1.School of Mining Engineering, College of Engineering, University of Tehran, Tehran, Iran.
2. Department of Mining Engineering, Faculty of Engineering, University of Birjand, Birjand, Iran

Article Info

Received 21 December 2023
Received in Revised form 26 March 2024
Accepted 12 April 2024
Published online 12 April 2024

DOI: 10.22044/jme.2024.13984.2609

Keywords

Block caving
Physical modeling
Numerical modeling
Base friction table
Height of caving zone

Abstract

The paper presents the effect of the dip of joints, joint spacing, and the undercutting method on the height of the caving in block caving. The obtained results show that among the three investigated parameters, respectively, the dip of joints, undercutting method, and joint spacing have the greatest effect on increasing the height of the caving zone. Comparing the data obtained from physical and numerical modeling shows a 97% match. Also, by increasing the joint spacing from 4 to 6 cm, 14%, from 6 to 8 cm, about 35%, and from 8 to 10, about 50%, the height of the caving zone has decreased. Regarding the dip of the joint, with the dip increasing from 30 to 45 degrees, about 3% of the caving height decreases. By increasing the dip of the joint from 45 to 60 degrees, the caving height has decreased by 42%. By increasing this value from 60 to 75 degrees, the caving height has increased by 50%. Also, changing the undercutting method from symmetric to advanced undercutting has increased the caving height by 40%. Additionally, three mathematical models have been proposed based on the shape of the caving zone in physical modeling.

1. Introduction

The mining industry has seen a significant increase in demand for ore production in recent years due to the development of societies and industrialization. As a result, the industry has been extracting from deep, low-grade, and massive mines. The block caving method has gained popularity due to its high production rate, low operating costs, high safety, and high mechanization capability[1]. Undercutting is excavated by constructing tunnels under the ore body in the block caving method. Then, by drawing the broken ore at the production/extraction level, a space is created, and due to gravitational and tectonic stresses, the roof gradually collapses, and the caving propagates [2].

Insufficient access to the ore body is one of the critical limitations in understanding the block caving method's mechanism. It leads to inadequate knowledge of the rock mass state under caving and the caving height profile. As a result, it becomes challenging to implement risk reduction measures and identify possible risks that can cause uncontrollable dynamic events on a large scale. Insufficient access to the deposit in this method can cause sudden collapse, undesirable fragmentation, and caving propagation outside the intended mining area, leading to a decrease in the ore grade [3,4].

The cavability of rock mass is the most critical parameter in the design of caving mines, which determines the possibility or impossibility of ore bodies to cave. The following important parameter is the height of the caving zone. These two parameters significantly impact other aspects of the design in this method [5]. Most of the recent studies have been about the evaluation of cavability. The

Corresponding author: amajdi@ut.ac.ir (A. Majdi)

history of cavability evaluation methods is fully mentioned by Alipenhani et al. [6-9]. Rafiee [10], [11] used a rock engineering system (RES), which analyzes the interrelationships between the effective parameters to study the cavability of rock. He also used a fuzzy system to minimize the subjectivity of weights calculated in the RES method. Raffie [12] has investigated the effect of seven parameters, the compressive strength of intact rock (UCS), joint orientation, joint persistence, joint density (P32), joint friction, confined stress, and hydraulic radius (HR) using numerical modeling. In order to assess the influence of each parameter in numerical modeling, the value of one parameter is changing while the values of other six parameters are fixed. The in-situ stress and hydraulic radius are the most effective parameters involved in cavability of rock mass in block caving mines.

Mohamadi et al. [13] have presented a hybrid probabilistically qualitative–quantitative model to evaluate cavability of immediate roof and to estimate the main caving span in longwall mining by combining the empirical model and the numerical solution. For this purpose, numerical simulation was incorporated to Roof Strata Cavability index (RSCi) as summation of ratings for nine significant parameters. A distinct element code was used to simulate numerically the main caving span corresponding to various RSCi classes probabilistically.

Alipenhani et al. [14] present the results of a comprehensive investigation of the applicability of various intelligence methods for optimal prediction of rock mass cavability in block caving by using effective geomechanical parameters.

Physical modeling can provide a handy tool to understand the complex mechanism of excavating in geomaterials under acceleration one “g” [15] and centrifugal loading [16] conditions. Physical modeling can be divided into three-dimensional and two-dimensional models. 3D physical models are usually expensive, time-consuming, and challenging to implement. However, three-dimensional models can be simplified by considering some assumptions and turning them into two-dimensional models, which are much easier to implement. The use of physical modeling in block caving research has been minimal. Most of these experiments focus on studying gravity flow and draw control. Several physical models can be found in the research background in which the block-caving process and the failure mechanism have been investigated [8]. Table 1 presents the history of the performed studies in the physical modeling field.

Due to the inaccessibility of the caving mass, engineers must rely on a perceptual model to design, instrument, model, and interpret how the caving propagates. Numerous researchers have conducted studies on the factors that impact the ability of a rock mass to cave. However, the primary aim of this paper is to achieve two objectives. Firstly, to establish a conceptual and representative physical model of the caving process, and secondly, to determine the impact of parameter interactions on the rock mass cavability using numerical, physical, and mathematical approaches. Previously, the process of caving using synthetic and jointed materials has not been physically modeled using the base friction table. Additionally, the estimation of caving height based on geometrical parameters of the joint has not been investigated using both physical and mathematical formulas. This paper discusses these topics.

The aim of this study is to investigate the impact of joint spacing, dip of joint, and undercutting method on caving zone height through constructing and conducting physical model tests. The base friction powder was used as modeling material for physical mode tests. Four modes (30 and 60), (45 and 45), (60 and 30), and (75 and 15) were chosen for the joint pattern. Four sizes of blocks, (3×5×4) cm, (3×5×6) cm, (3×5×8) cm, and (3×5×10) cm, are considered to investigate the effect of spacing on the height of the caving zone. The effect of the undercutting method on caving height was investigated using two methods, symmetrical undercutting and advanced undercutting. Also, this study used numerical modeling to validate the results obtained from the physical modeling. The UDEC software is used for numerical modeling. The schematic flowchart of the present research methodology is depicted in Figure 1.

Table 1. History of physical modeling used in cavability assessment

Model type	References	Purpose and application
Physical modeling	Park and Kicker [17]	Study of the stress distribution around chain pillar in the longwall method
	Whittaker [18]	Study of mining-induced subsidence by the longwall method, and investigation of the fractures at the upper floors of the stope
	McNEARNY and ABEL [19]	Study of draw behavior of jointed rock mass in the block caving method
	Carmichael and Hebblewhite[3]	Analysis of crack propagation and the areas formed in the large caving extraction method
	Potvin[20]	Analysis of the caving mechanism under the plane strain conditions in a centrifuge experiment
	Jacobsz and Kearsley [21]	In a centrifuge experiment, the results of placing a weak mass of artificial rock under high and low horizontal stress conditions were examined.
	Bai *et al.*[22]	In this study, experiments were performed on two large-scale physical models including sand, gravel, gypsum, and mica to investigate the cavability of top coal with hard rock bands based on two real cases.
	Khosravi *et al*. [23]	Investigation of caving mechanism in the block caving method using numerical and physical modeling

Figure 1. Schematic flowchart of present research methodology

2. Test platform

Goodman [23] presented the principles of the base friction table, in which he simulated the earth's gravity with a frictionsal force created between the moving friction surface of the table and the model. Nishida et al. [24] built a base friction table to study the propagation of subsidence in Japan.

The base friction table used in this study is shown in Figure 2. On the solid metal plate of the table, a belt is placed. The table moves horizontally along the “Y” axis. It rotates the rotation of the driving axes connected to an electric motor in an endless cycle. The goal is to convert the vertical section of the undercut into a two-dimensional model in this device.

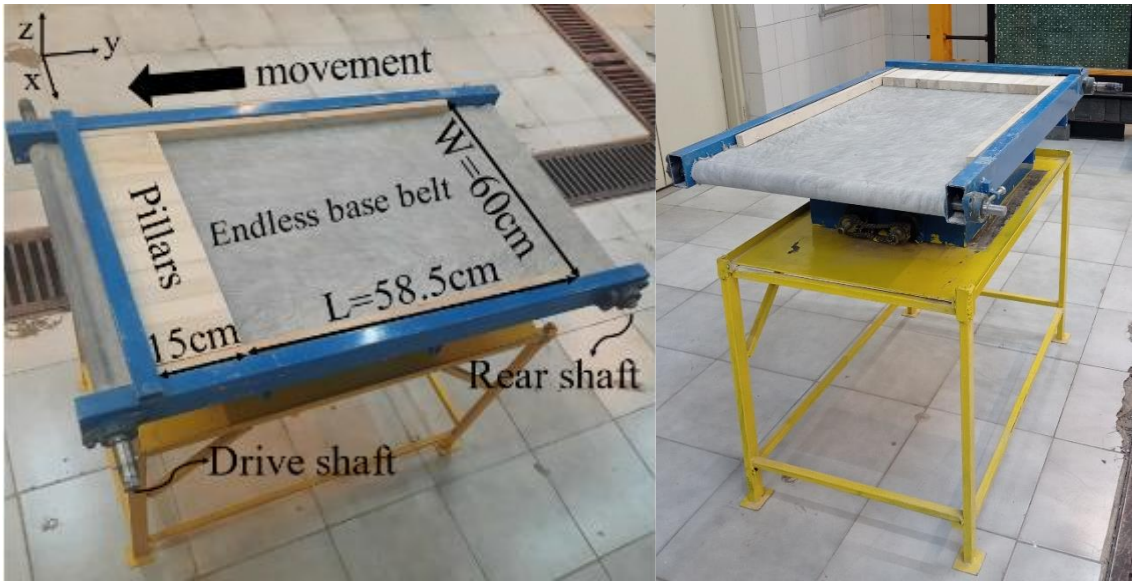

Figure 2. Base friction table used for physical modeling of the caving process

The physical model with a thickness of 30 mm is placed on the base belt. After creating the undercut span and moving the belt, the caving propagates. Bearing in mind that the upper surface of the model is free and prone to vertical movement (Figure 2).

In the base friction table, the displacement of the bottom of the model is limited, and with the movement of the base belt, the friction force F is created between the base belt and the bottom of the model. This friction force can be calculated as follows:

$$F = \gamma_m \times t \times \mu \times A \quad (1)$$

where:

F: Frictional force between the base belt and the bottom of the model (kN)

$\boldsymbol{\gamma_m}$**:** Unit weight of materials used in the model (kN/m^3)

t: model thickness (m)

$\boldsymbol{\mu}$ **:** coefficient of friction between the model and the base belt

A: Area of the floor area of the model (m^2)

According to Hei et al. [25], the model's thickness should be limited in the simulation of gravity stress in the model that uses the applied force F. As the force of gravity operates in the center of the model, while the applied force F is distributed across all areas of the model.

Blocks of wood with dimensions of 150×40×30 mm were placed in the lower part of the model as a base (Figure 3), which simulates the process of undercutting by removing these blocks. As shown in Figure 3, after each stage of undercutting, the base belt moves at a constant speed until the caving height reaches a constant value. Figure 3 shows an example of the stages of an experiment along with the investigated parameters. In the actual block caving operation, one of the solutions to facilitate the caving is to excavate slots in the boundaries of the ore body (through fan drilling). In the present physical model, no horizontal stress has been applied to the model, and the boundaries have been fixed.

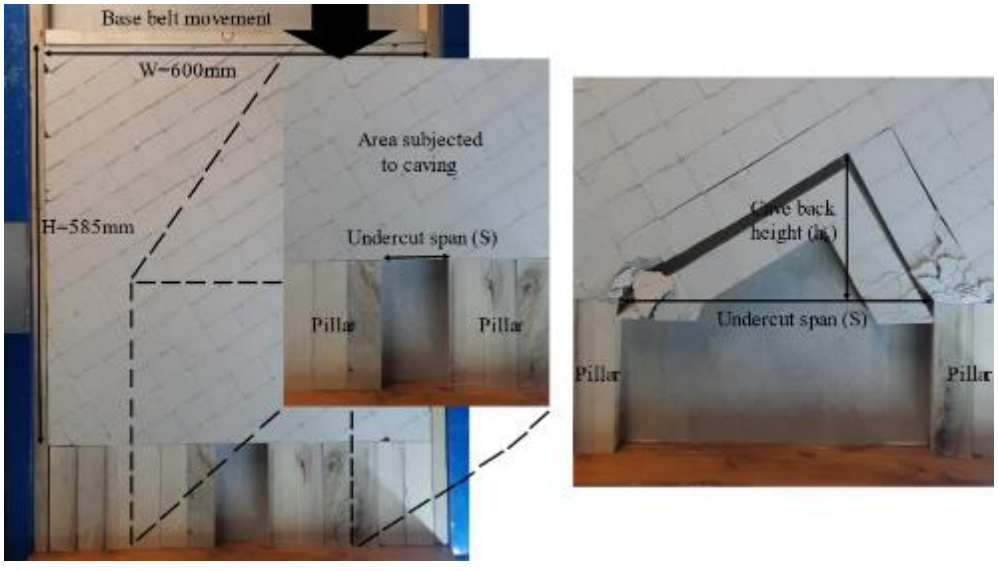

(a) **(b)**

Figure 3. Physical model components and parameter's definition: (a) prepared model and (b) failure due to undercutting

3. Material sample

Various mixtures of materials have been used in physical modeling with a base friction table in previous studies. One such mixture was used by Goodman, who combined flour, liquid oil, and sand in his experiments. Nishida et al. [24] used a mixture of BaSo4, ZnO, and Vaseline oil in their physical model, with a 9:21:70 mass ratio. This mixture, called the base friction powder, has been widely accepted and used in other studies, such as [25] and [26], with satisfactory results. Therefore, for this study, the base friction powder was chosen as the material for the physical model. This powder can be compressed to create blocks with specific weights and required strength. The mechanical and physical properties of the powder were evaluated through various experiments conducted by [20] to assess the results of the physical models [26]. Table 2 presents the characteristics of the materials used.

Table 2. Mechanical and physical properties of the physical block models and base friction powder [26]

Material	Unit Weight (kN/m^3)	UCS (kPa)	Modulus of Elasticity (MPa)	Poisson's ratio	Tensile Strength (kPa)	Friction Angle (Degree)	Cohesion (kPa)
Block	19.33	46	7	0.26	25	31	13
Powder	14	*	3	0.25	0	20	0.35

To investigate the effect of joint spacing on the height of the caving zone, blocks made of base friction powder in four different sizes: 10×5×3 cm, 8×5 ×3 cm, 6×5×3 cm and 4×5×3 were prepared. These blocks are shown in **Figure 4**.

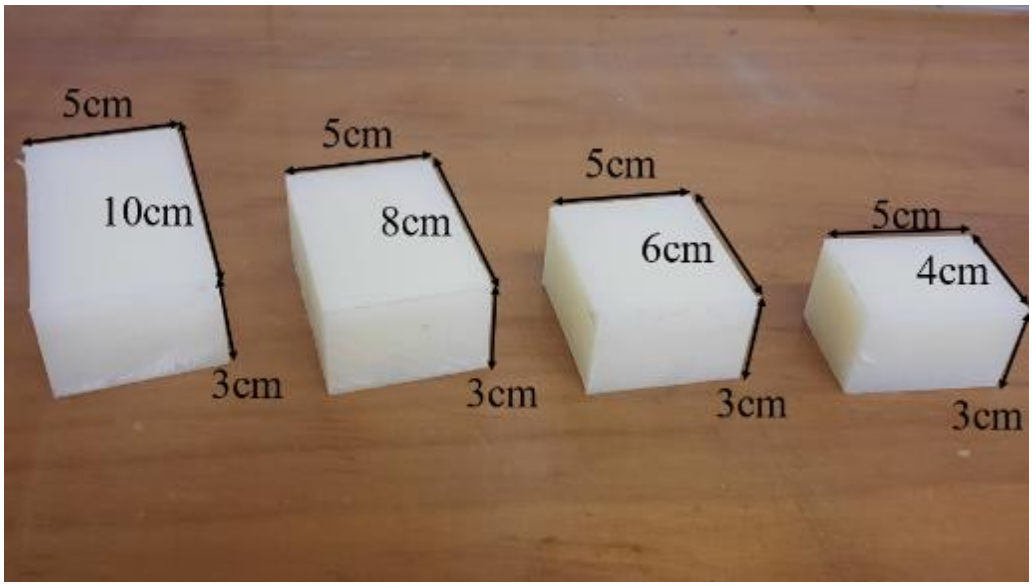

Figure 4. Blocks with different dimensions have been prepared for required physical models

4. Physical model testing

In this study, the effect of three parameters, the dip of the joint, spacing of the joint, and the method of undercutting on the height of the caving zone, has been investigated. For this purpose, a series of physical tests with a combination of different situations were performed for these three parameters, and the height of caving was measured. Measurement of the height of the caving was done by photographing the model and using AutoCAD software.

The assumptions of physical modeling are as follows:

1) The model is not subjected to horizontal stress, and only the sides of the model are fixed.
2) The blocks are moved in the x and y directions, and there is no movement in the direction perpendicular to the plane.
3) The rotation of the belt will continue until there is no change in the condition of the model by rotating the belt

If the lower right corner of the model is considered as the origin of the coordinates and the direction of rotation is clockwise, four modes of 30 and 60 degrees, 45 and 45 degrees, 60 and 30 degrees, and 75 and 15 degrees are selected for the joint pattern. These modes are shown in Figure 5.

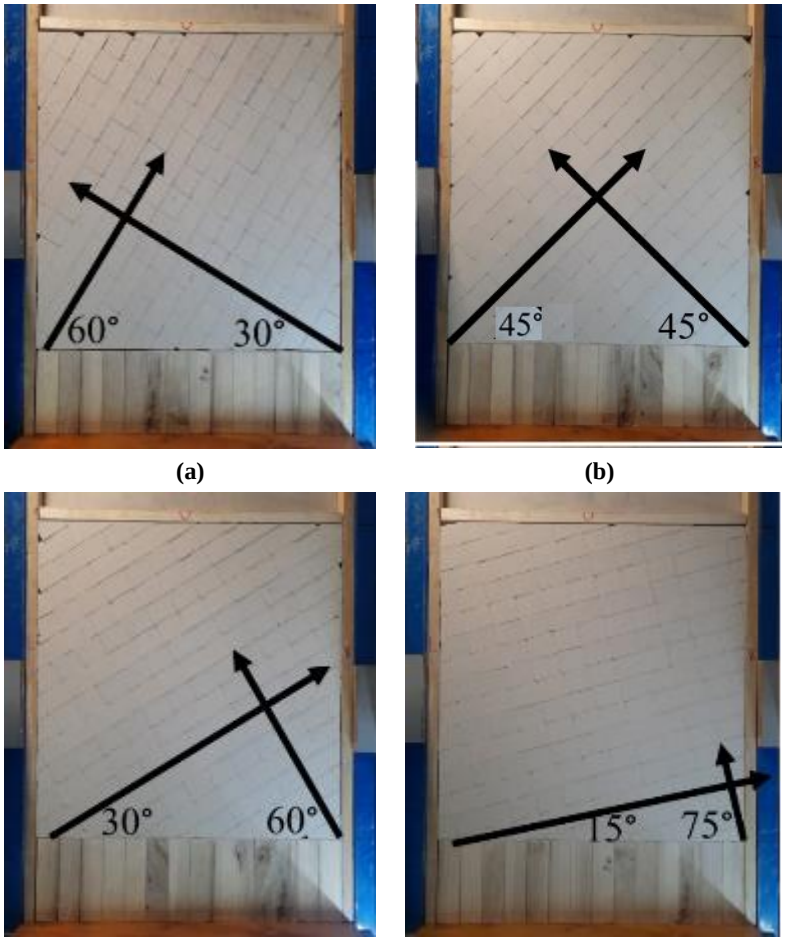

(a) (b) (c) (d)

Figure 5. Joint sets pattern in the physical model: a) 30 and 60 degrees, b) 45 and 45 degrees, c) 60 and 30 degrees, d) 75 and 15 degrees

Also, two undercutting methods were investigated to study the effect of undercutting on the height of the caving zone, which are explained below.

a) **Symmetric undercutting method:** The undercutting operation starts by creating a 4 cm span in the model's center, and the base belt moves at a constant speed. This movement of the belt continues until a constant caving height is created. The constant height of the caving means no change in this parameter with the rotation of the base belt. Then the undercut is increased symmetrically and with steps of 8 cm (one wooden pillar is removed from the right side, and one is removed from the left side). This process continues until the height of the caving reaches the upper level of the model or the stress on the remaining pillars of the materials on both sides increases to such an extent that the blocks break. This process is shown in Figure 6 for 4×5×3 cm blocks. In this figure, h_c is the height of the caving zone in centimeters, and S is the span width of the undercut in centimeters.

b) **Advanced method:** In this method, the undercut operation starts with a 4 cm span on the right side of the model, and the base belt moves at a constant speed until a constant caving height is formed. Then the undercut moves to the left side of the model with 4 cm steps. This process continues until the caving reaches to a height where the transferred stresses over the remaining pillars increase to such an extent that the blocks in front of them fail. The caving process in advanced mode is shown in Figure 7 for 10×5×3 cm blocks and the joint sets with inclination angles.

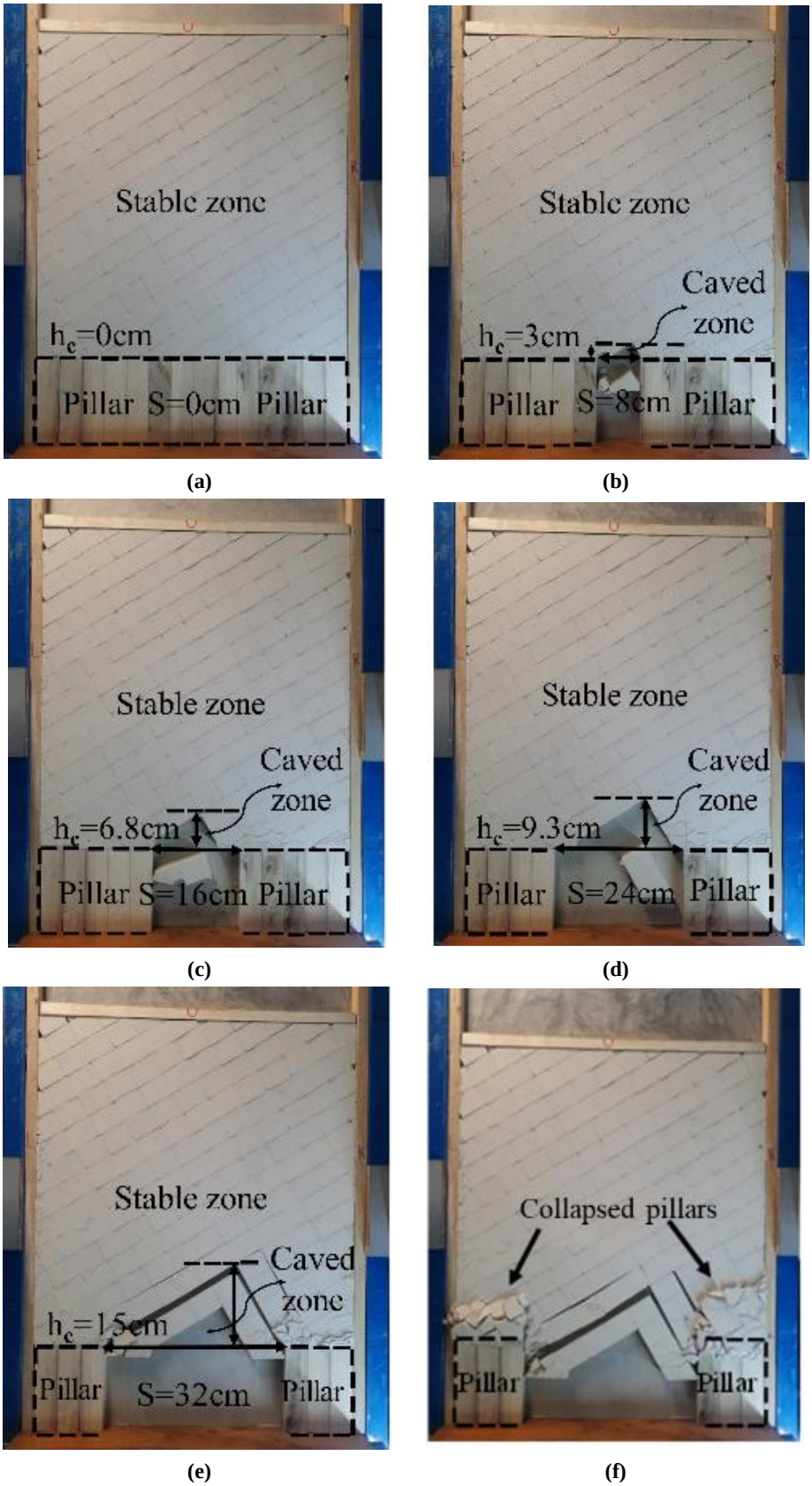

Figure 6. Caving process in symmetrical undercutting method a) span=0, b) span=8cm, c) span=16cm, d) span=24cm, e) span=32cm, f) breaking the rib pillars.

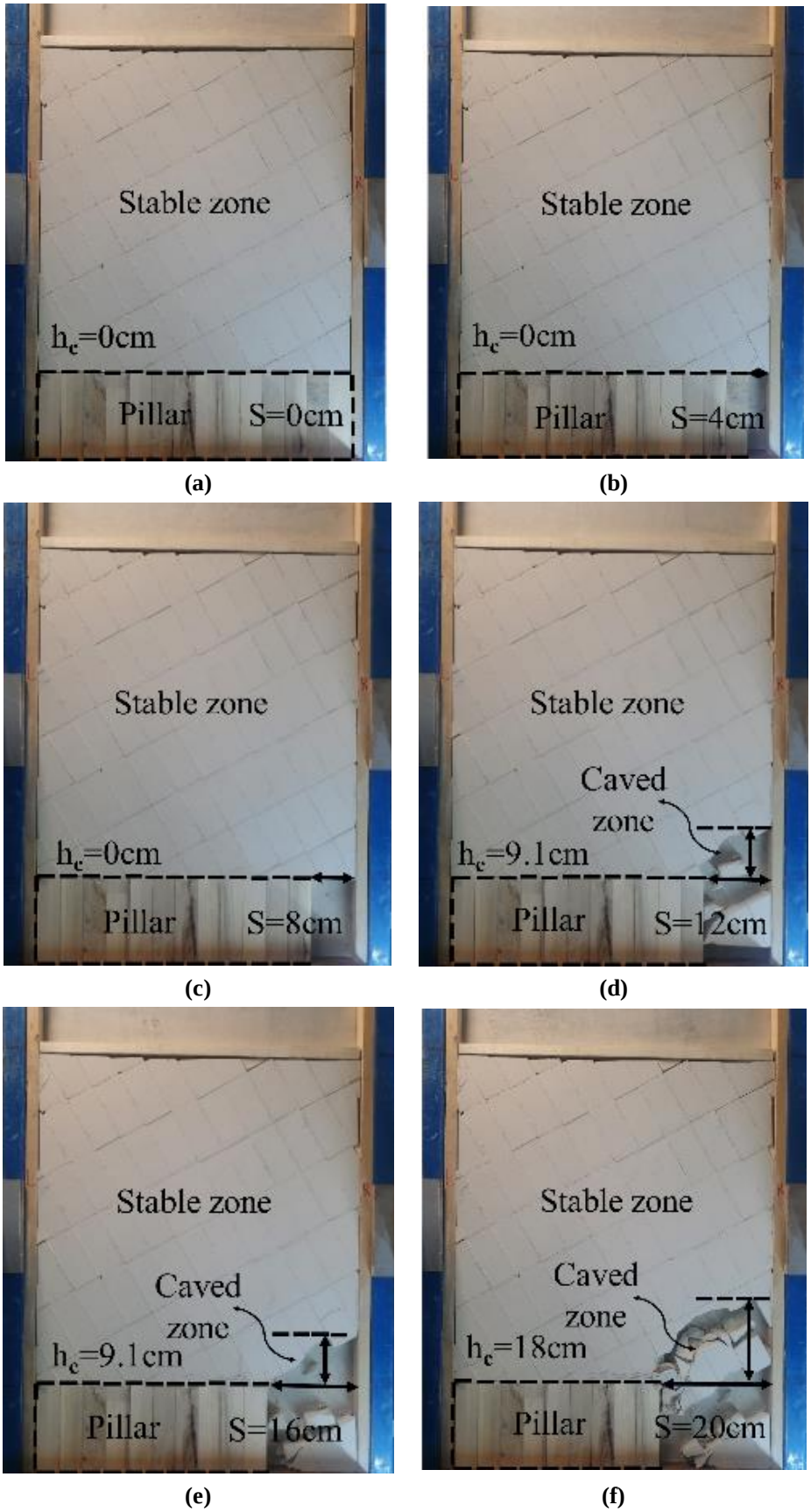

Figure 7. Caving process in symmetrical undercutting method a) span=0, b) span=4cm, c) span=8cm, d) span=12cm, e) span=16cm, f) span=20cm, g) span=24cm, h) span=28cm, i) span=32cm, j) span=36cm,

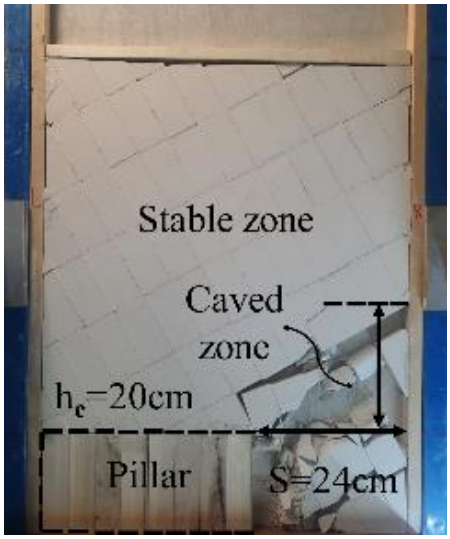

(g)

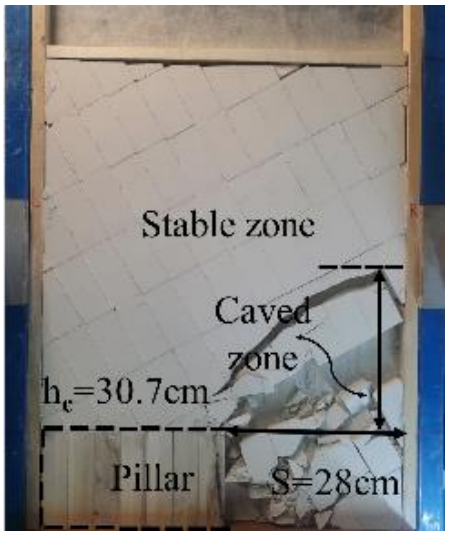

(h)

(i)

(j)

(k)

Continuous of Figure 7. Caving process in symmetrical undercutting method a) span=0, b) span=4cm, c) span=8cm, d) span=12cm, e) span=16cm, f) span=20cm, g) span=24cm, h) span=28cm, i) span=32cm, j) span=36cm, k) breaking the rib pillars.

4.1. Experimental design with Taguchi method

Taguchi proposed a method to optimize industrial processes. This method examines the system's output response to changes in different interrelated parameters in some modes. The method is based on statistical analysis that analyzes the sensitivity of the target variables to the input variables to improve the quality of the result. The effect of each parameter on the system in the Taguchi method is similar to the signal/noise ratio.

To optimize the number of tests, the Taguchi test design method was used in Minitab software. This software can simultaneously check several responses with different characteristics and provide various statistical charts. In this method, the parameters and levels are determined first. Table 3 shows the different levels of the three independent parameters examined. Then, using the Minitab software, orthogonal arrays were designed (Table 4). L16 array is used in this research.

Table 3. Taguchi method parameters

Number	Parameter	Level 1	Level 2	Level 3	Level 4
1	Joint spacing (cm)	4	6	8	10
2	Dip of the joint (degree)	30	45	60	75
3	Undercutting method	Symmetric	Advanced	*	*

Table 4. L16 Taguchi orthogonal table

Test number	Joint spacing (cm)	Dip of the joint (degree)	Undercutting method
1	4	30	Advanced
2	4	45	Advanced
3	4	60	Symmetric
4	4	75	Symmetric
5	6	30	Advanced
6	6	45	Advanced
7	6	60	Symmetric
8	6	75	Symmetric
9	8	30	Symmetric
10	8	45	Symmetric
11	8	60	Advanced
12	8	75	Advanced
13	10	30	Symmetric
14	10	45	Symmetric
15	10	60	Advanced
16	10	75	Advanced

4.2. Results and discussion

As was said before, this study aims to investigate and analyze the effect of three parameters of dip, joint spacing, and undercutting method on the height of the caving zone. By conducting experiments and measuring the height of the caving zone in each experiment, using Minitab software and Taguchi analysis, a table and graph of the signal-to-noise ratio of the data can be plotted. Table 5 shows the values of each parameter's signal-to-noise ratio.

In Table 5, it is clear that among the three investigated parameters, the dip, undercut method, and joint spacing have the greatest effect on the caving height, respectively.

The table presented below displays the signal-to-noise values for each parameter at different levels. A higher value indicates a greater impact of that parameter on the objective function, i.e., minimum caving span. Based on the results, the importance of the investigated parameters is in the following order: the dip of the joint, the method of undercutting, and the spacing of the joint. These results are also represented in a diagram in Figure 8.

Table 5. Response table for signal to noise ratios

Level	Joint spacing (cm)	Dip of joint (Degree)	Undercutting method
1	32.39	30.95	32.32
2	30.96	31.23	27.43
3	28.44	25.73	
4	27.69	31.57	
Delta	4.69	5.84	4.89
Rank	3	1	2

Also, the signal-to-noise ratio diagram (Figure 8) shows the effect of the parameters on the caving height. Regarding the joint spacing parameter, it is clear that the highest caving zone is obtained in the joint spacing of 4 cm, and as the joint spacing increases, the height of the caving decreases. Blocks with a joint spacing of 4 and 6 cm have a relatively positive effect on increasing the height of the caving. Blocks with a spacing of 8 and 10 will reduce the relative height of the caving. The highest caving height occurs at the 75-degree dip of the joint. The caving height is affected by the angles used in the undercutting process. Angles of 75, 45, and 30 degrees have a positive impact on the height of the caving, while an angle of 60 degrees results in a relative decrease. Additionally, the advanced undercutting method leads to a relative increase in caving height, whereas the symmetrical undercutting method leads to a relative decrease.

At a 70-degree slope, the driving force (sinusoidal component compared to gravity's sinusoidal component) increases. On slopes close to vertical, the most important factor is the friction angle of the joint surface.

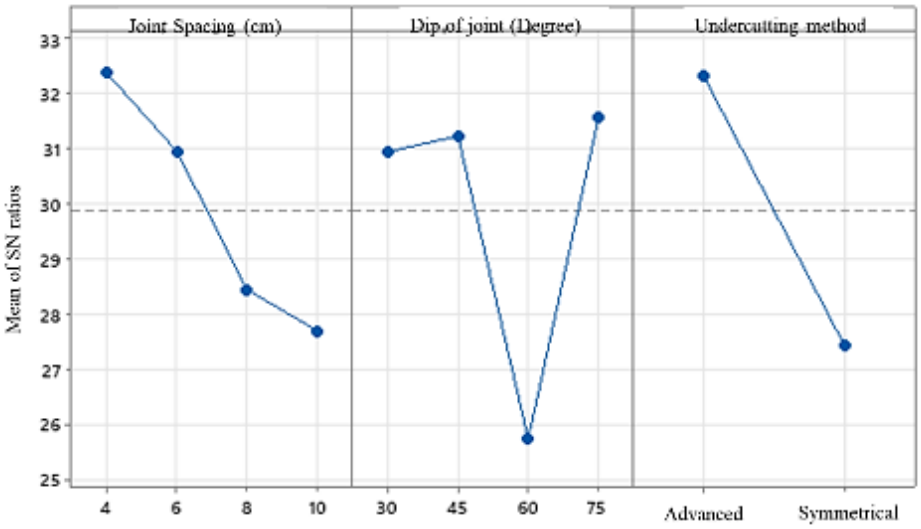

Figure 8. Plot for signal to noise ratios

Figure 9 illustrates the counter plot of joint dip angle versus joint spacing. It can be seen that the highest caving height (50 m and up) occurs in the range of joint spacing of 4 to 7 cm related to joint dip angles 30 up to 52 degrees and within the joint spacing of 4 to 5.5 cm and joint dip angle higher than 73 degrees as well.

In the first area, due to limited spacing and a more jointed environment, cracks in the blocks result in less border locking, increasing the likelihood of caving. But in the second one, due to the increase of the dip angle, this parameter will play a more effective role in increasing the height of caving so that in the angle of 90 degrees, the controlling parameter of the height of caving is the angle of the joint.

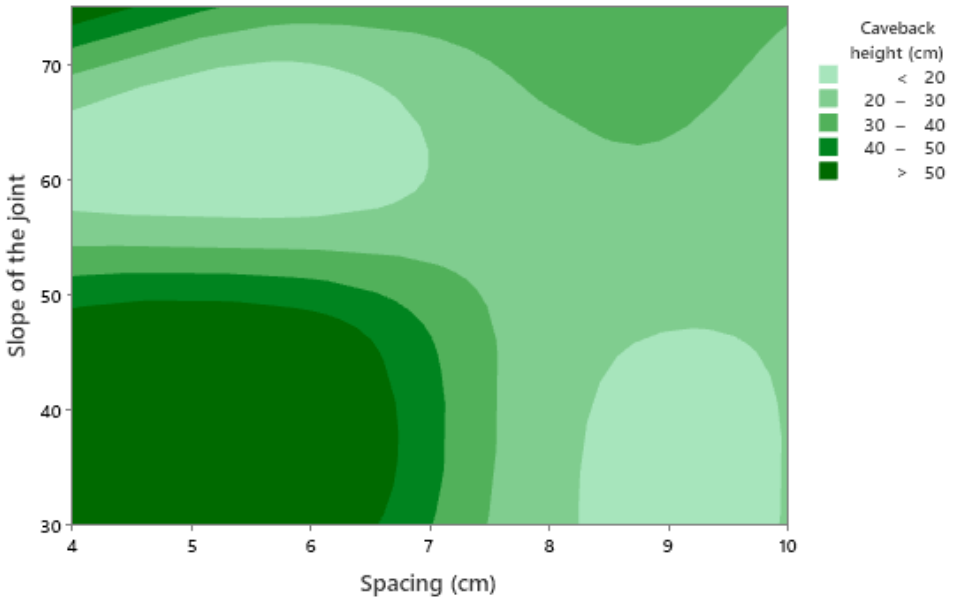

Figure 9. Contour plot of cave back height vs dip of joint, joint spacing

5. Numerical modeling

To validate the data obtained from physical modeling, UDEC software [27] was used. This software is a two-dimensional numerical program based on the discrete element method for discontinuous environments. It is obvious that for implementing numerical modeling, the physical and mechanical properties of the block materials must be available (Table 6). The Mohr-Coulomb criterion is used in this numerical model. The Voronoi model was used to simulate a failure, and the parameters of this model were similar to the geomechanical parameters of the physical models.

The results of the numerical simulation of the physical model in the UDEC software for 4×5×3 cm blocks, the dip of joints 60 and 30 degrees, and symmetrical undercutting are shown in Figure 10. Also, the results for the block size 10×5×3 cm, the dip of joint 60 and 30 degrees, and advanced undercutting are shown in Figure 11.

Table 6. Input data for numerical model

Model parameters	Block	Voronoi model	Joint
Unit Weight (kN/m3)	19.33	*	*
Modulus of Elasticity (Mpa)	7	*	*
Poisson's ratio	0.26	*	*
Tensile Strength (Kpa)	25	25	0
Friction Angle (degree)	31	31	13
Cohesion (Kpa)	13	13	0
Normal stiffness (Mpa/m)	*	50	5
Shear stiffness (Mpa/m)	*	20	2

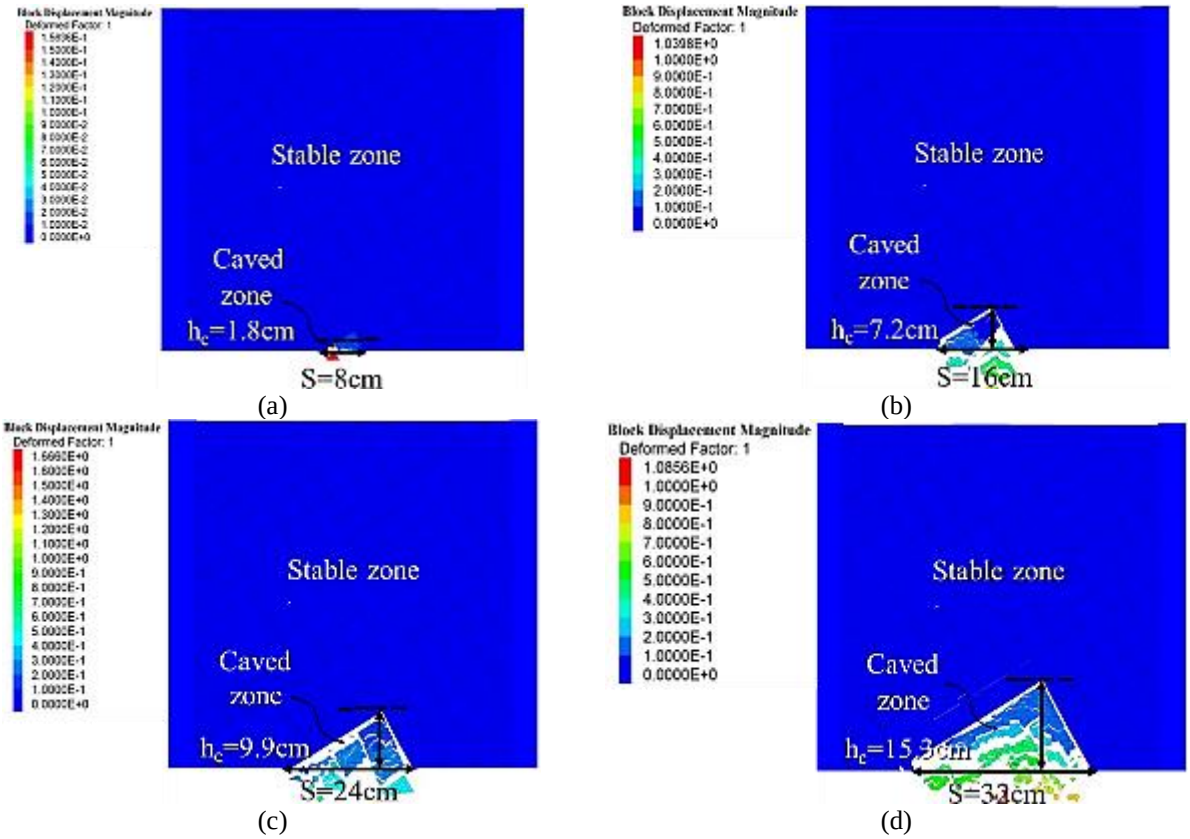

Figure 10. Simulation of caving process in symmetrical undercutting method a) span=8cm, b) span=16cm, c) span=24cm, d) span=32cm.

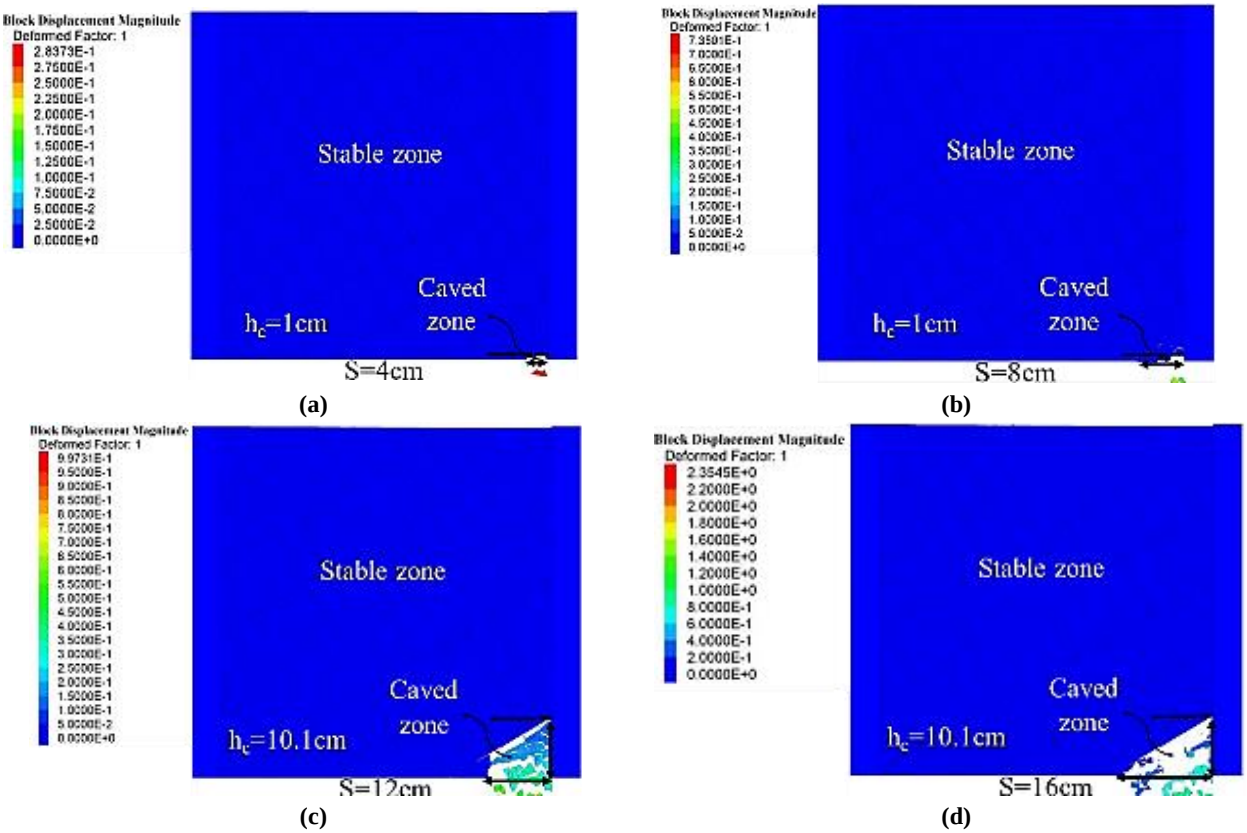

Figure 11. Simulation of caving process in symmetrical undercutting method a) span=4cm, b) span=8cm, c) span=12cm, d) span=16cm, e) span=20cm, f) span=24cm, g) span=28cm, h) span=32cm, i) span=36cm.

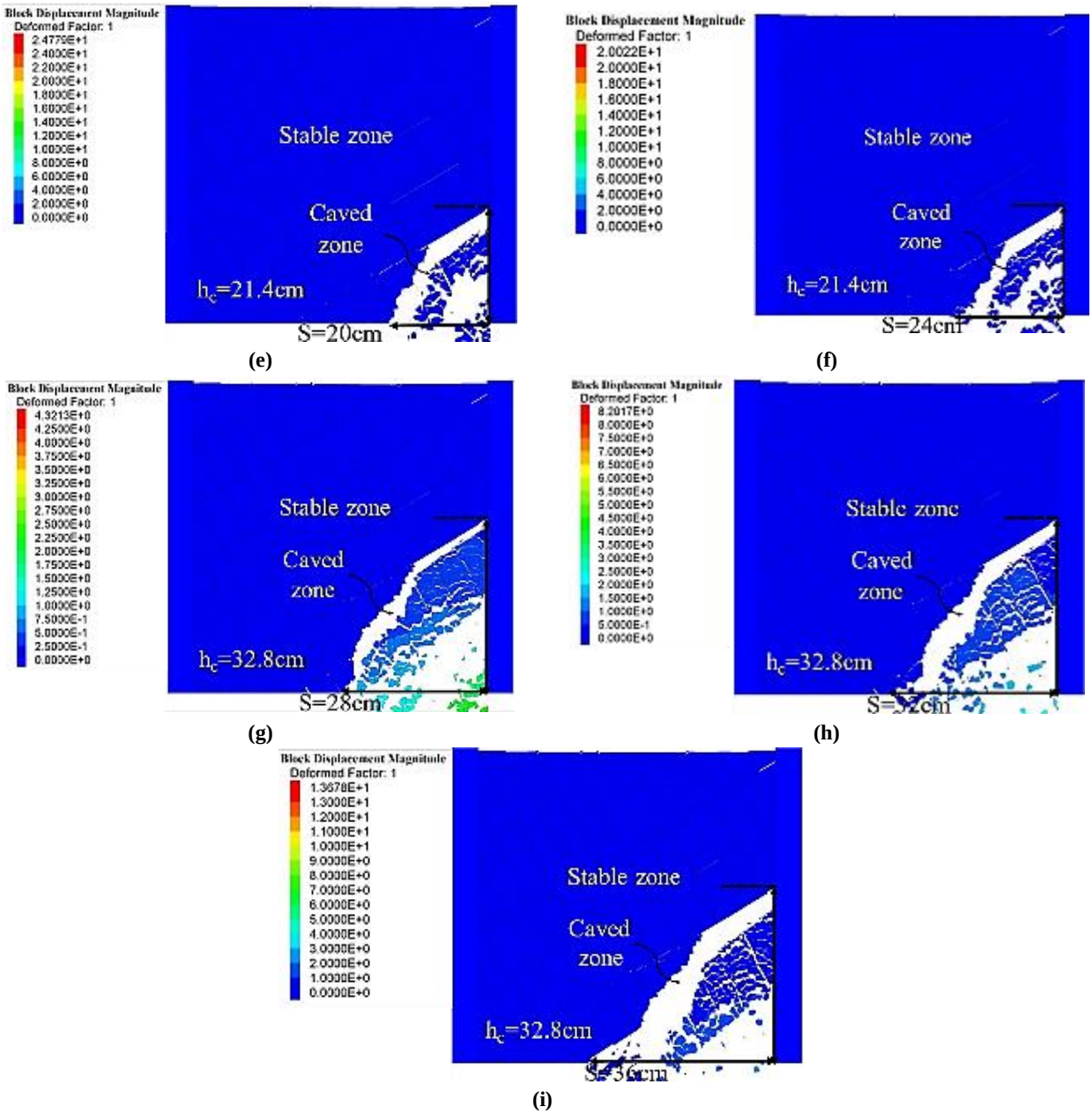

Continuous of Figure 11. Simulation of caving process in symmetrical undercutting method a) span=4cm, b) span=8cm, c) span=12cm, d) span=16cm, e) span=20cm, f) span=24cm, g) span=28cm, h) span=32cm, i) span=36cm.

Comparison of the Physical and numerical modeling's results based on 16 different combinations of the three parameters given in Table 4 shows a very good accord between the two modeling methods (Figure 12 to Figure 17). This means that there is a good match between the physical and numerical modeling results in terms of the caving zone shape and height.

A better comparison of the shape and the height of the caving zone and the final shape of the caving area in physical modeling for all modes is presented in Figure 12 to Figure 15. The shape of the caving zone induced by the physical models is fairly compatible with that produced by the numerical modeling. As evident from the figures, both the numerical and physical models show a nearly identical shape of the caved and displaced area, with very similar heights as well. The comparative diagrams of the height of caving zone have been shown in Figures 16 to 19.

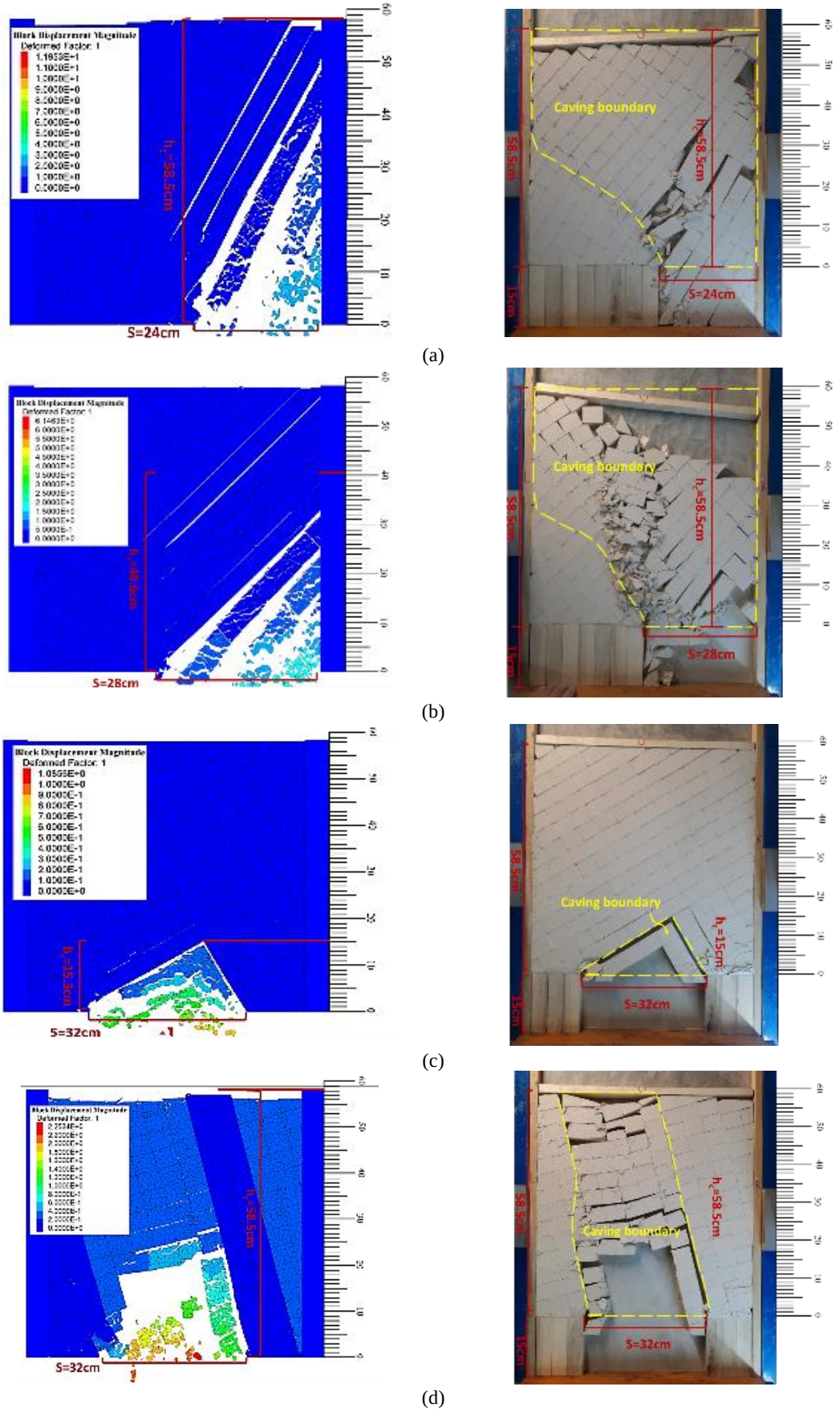

Figure 12. Comparing the results of physical and numerical modeling for the final undercut span in the size of a 4cm block: a) 30 and advanced undercutting, b) 45 and advanced undercutting, c) 60 degree and symmetrical undercutting, d) 75 and symmetrical undercutting.

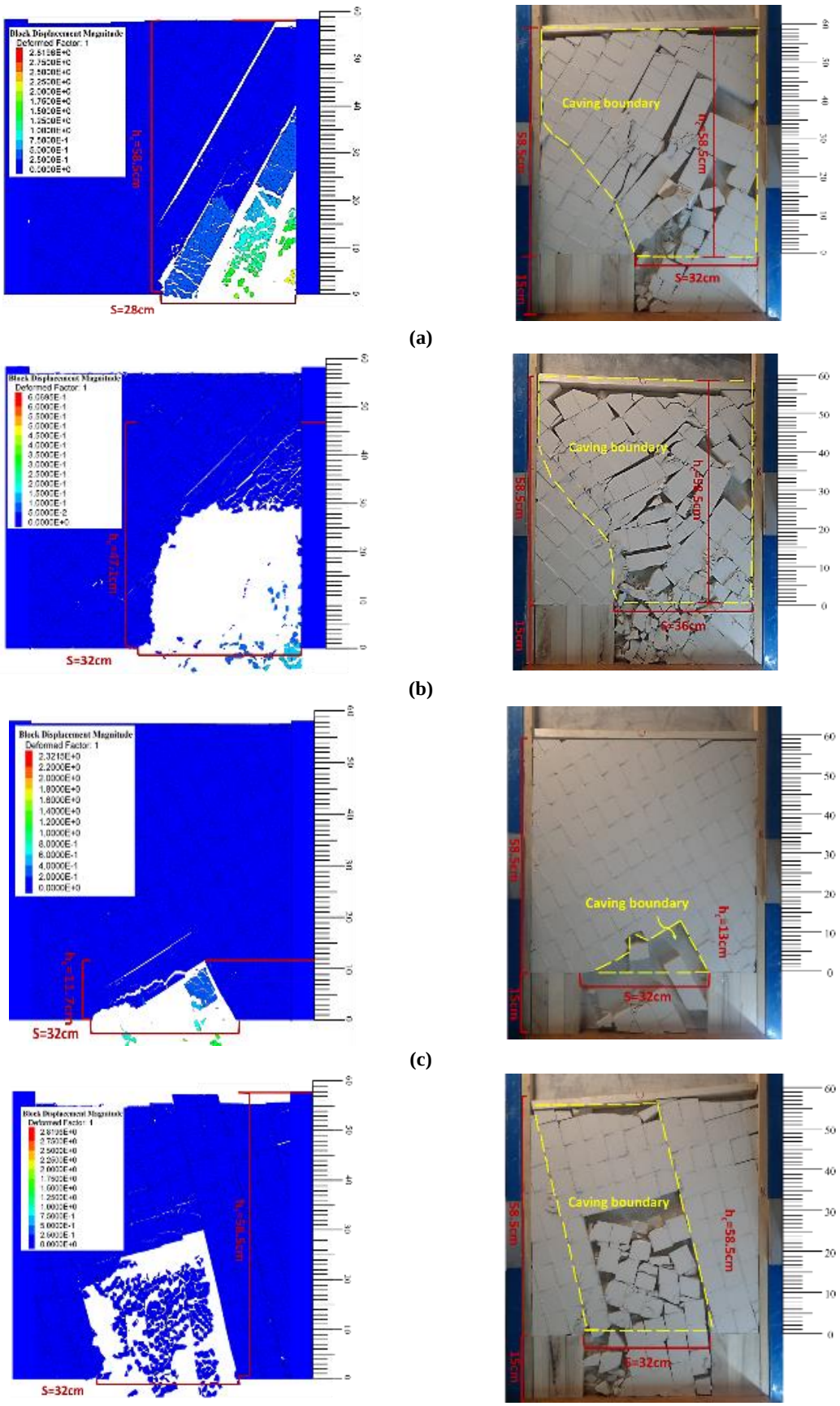

Figure 13. Comparing the results of physical and numerical modeling for the final undercut span in the size of a 6cm block: a) 30 and advanced undercutting, b) 45 and advanced undercutting, c) 60 and symmetrical undercutting, d) 75 and symmetrical undercutting.

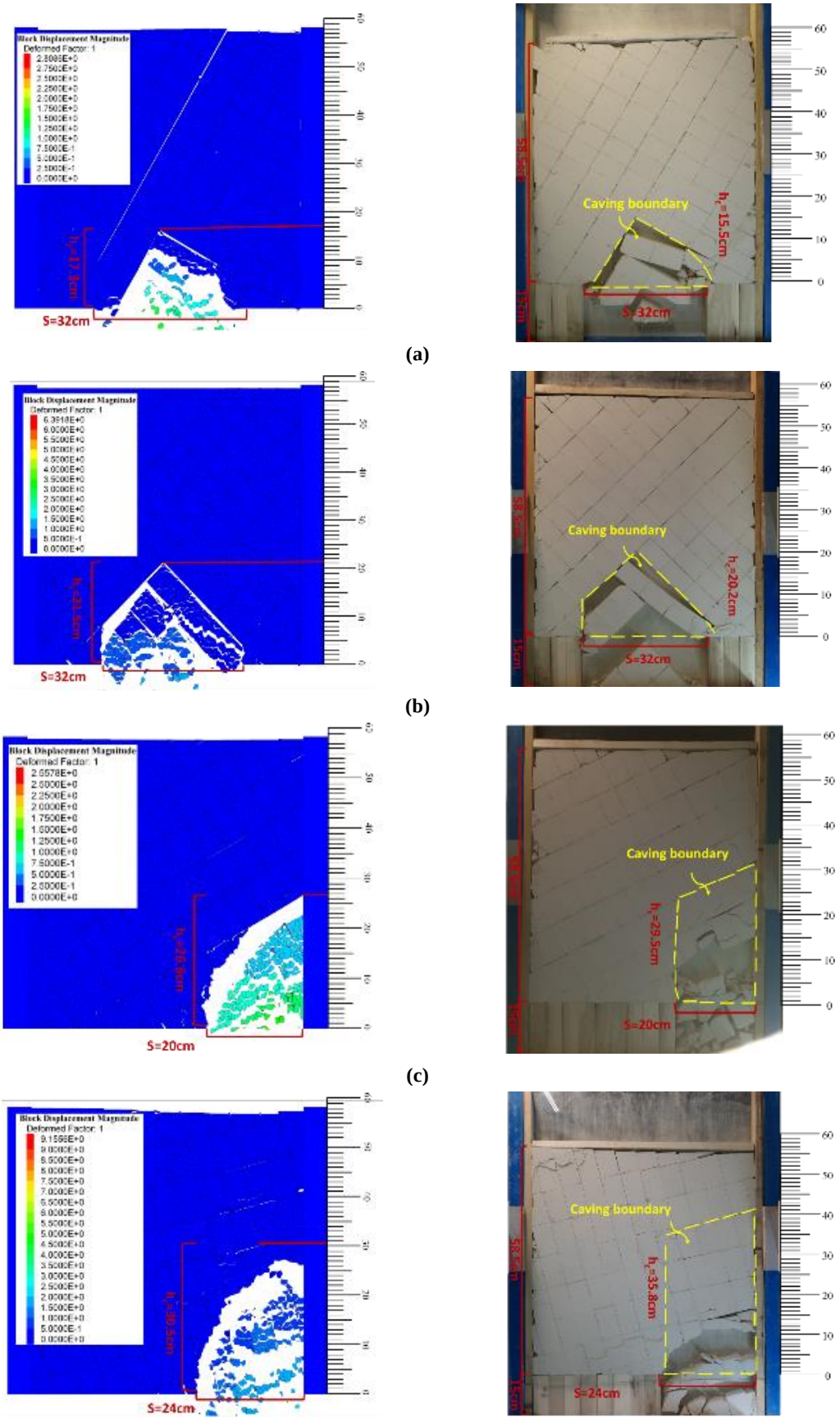

(a)

(b)

(c)

(d)

Figure 14. Comparing the results of physical and numerical modeling for the final undercut span in the size of a 8cm block: a) 30 and symmetrical undercutting, b) 45 and symmetrical undercutting, c) 60 and advanced undercutting, d) 75 and advanced undercutting.

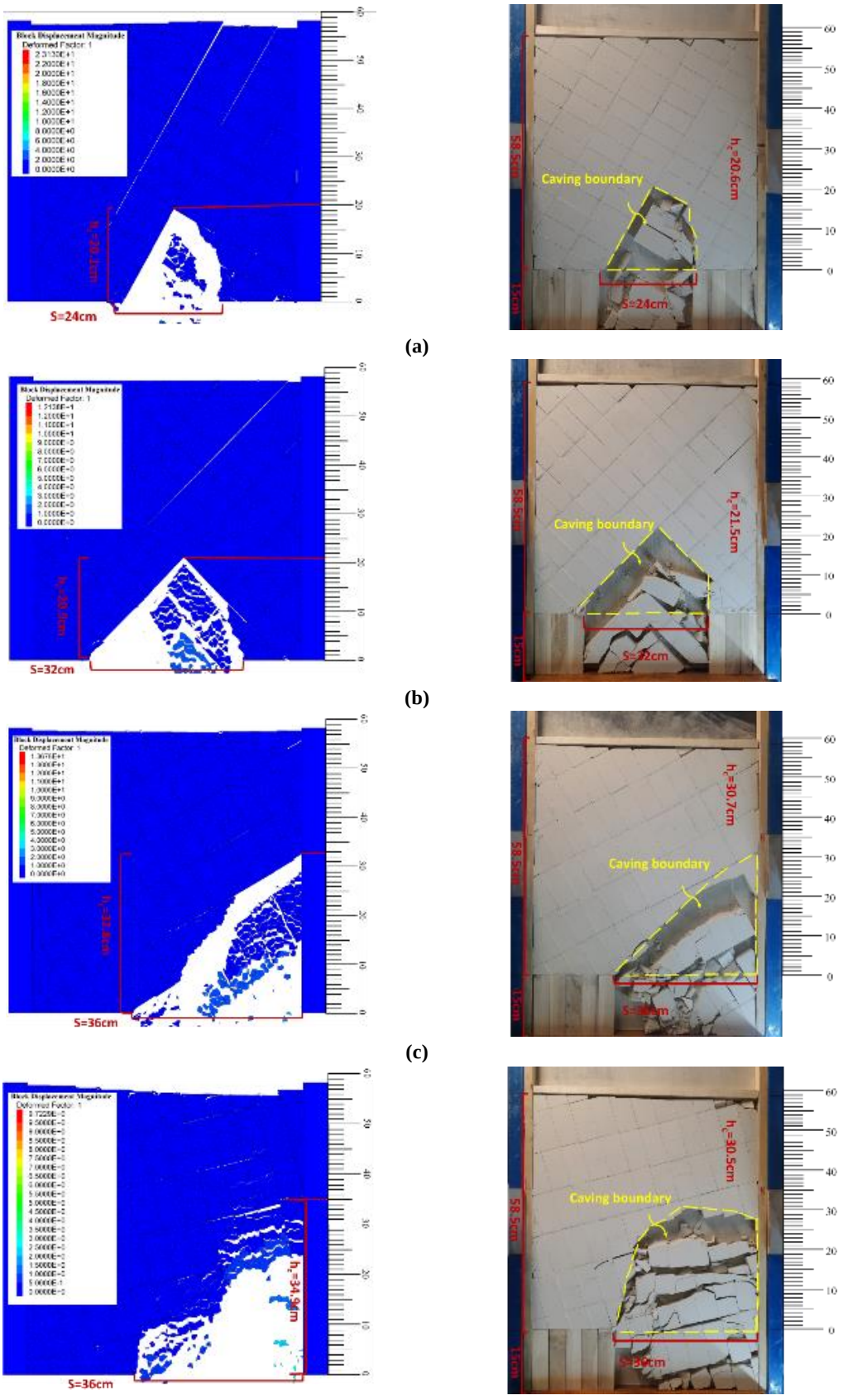

Figure 15. Comparing the results of physical and numerical modeling for the final undercut span in the size of a 10cm block: a) 30 and symmetrical undercutting, b) 45 and symmetrical undercutting, c) 60 and advanced undercutting, d) 75 and advanced undercutting.

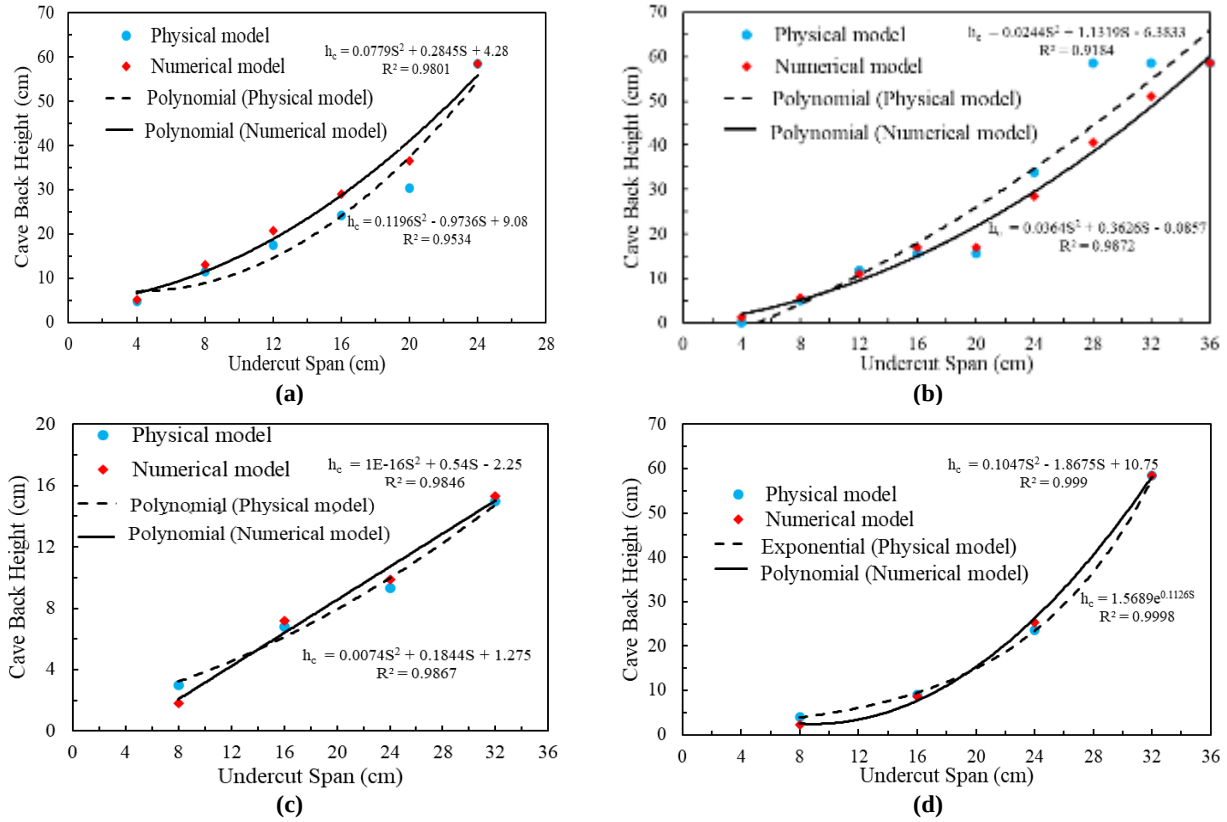

Figure 16. Comparing the results of physical and numerical modeling for size of a 4cm block: a) 30 and advanced undercutting, b) 45 and advanced undercutting, c) 60 and symmetrical undercutting, d) 75 and symmetrical undercutting.

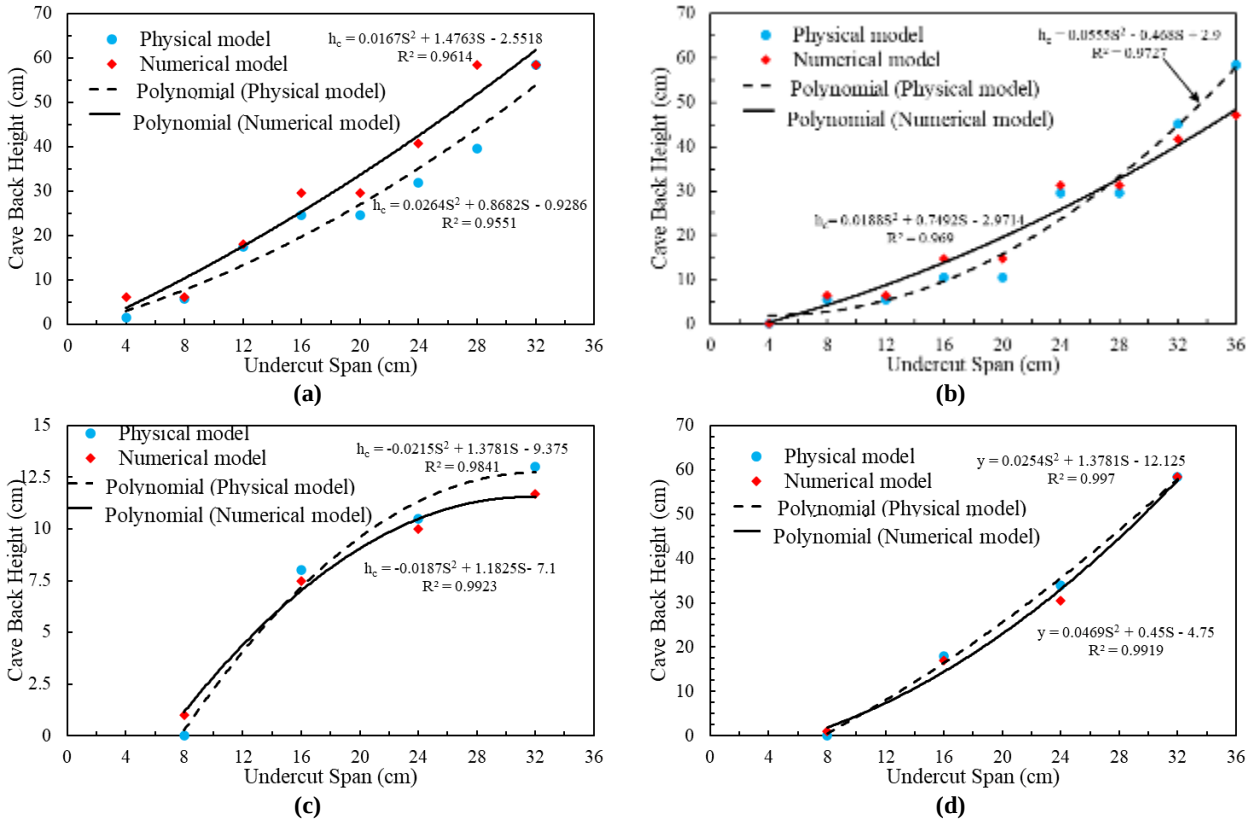

Figure 17. Comparing the results of physical and numerical modeling for size of a 6cm block: a) 30 and advanced undercutting, b) 45 and advanced undercutting, c) 60 and symmetrical undercutting, d) of 75 and symmetrical undercutting.

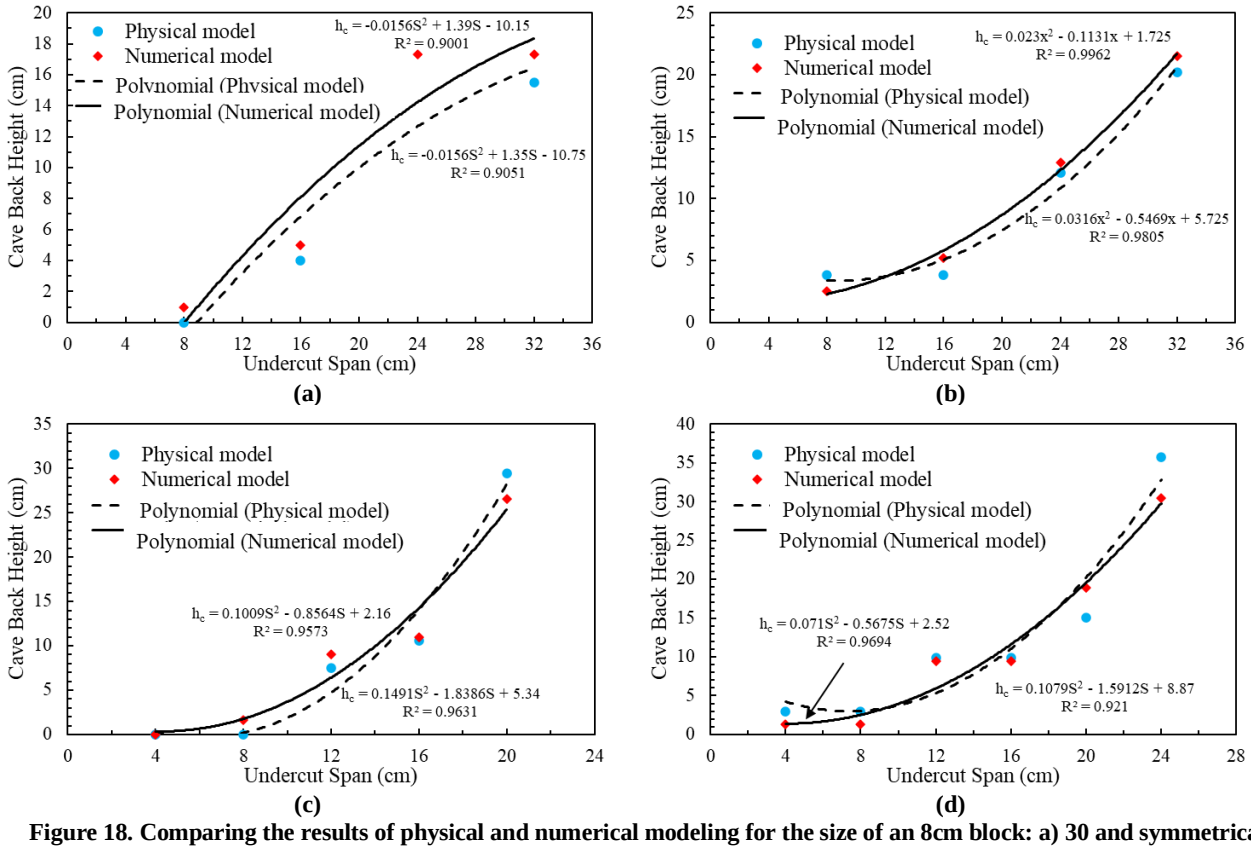

Figure 18. Comparing the results of physical and numerical modeling for the size of an 8cm block: a) 30 and symmetrical undercutting, b) 45 and symmetrical undercutting, c) 60 and advanced undercutting, d) 75 and advanced undercutting.

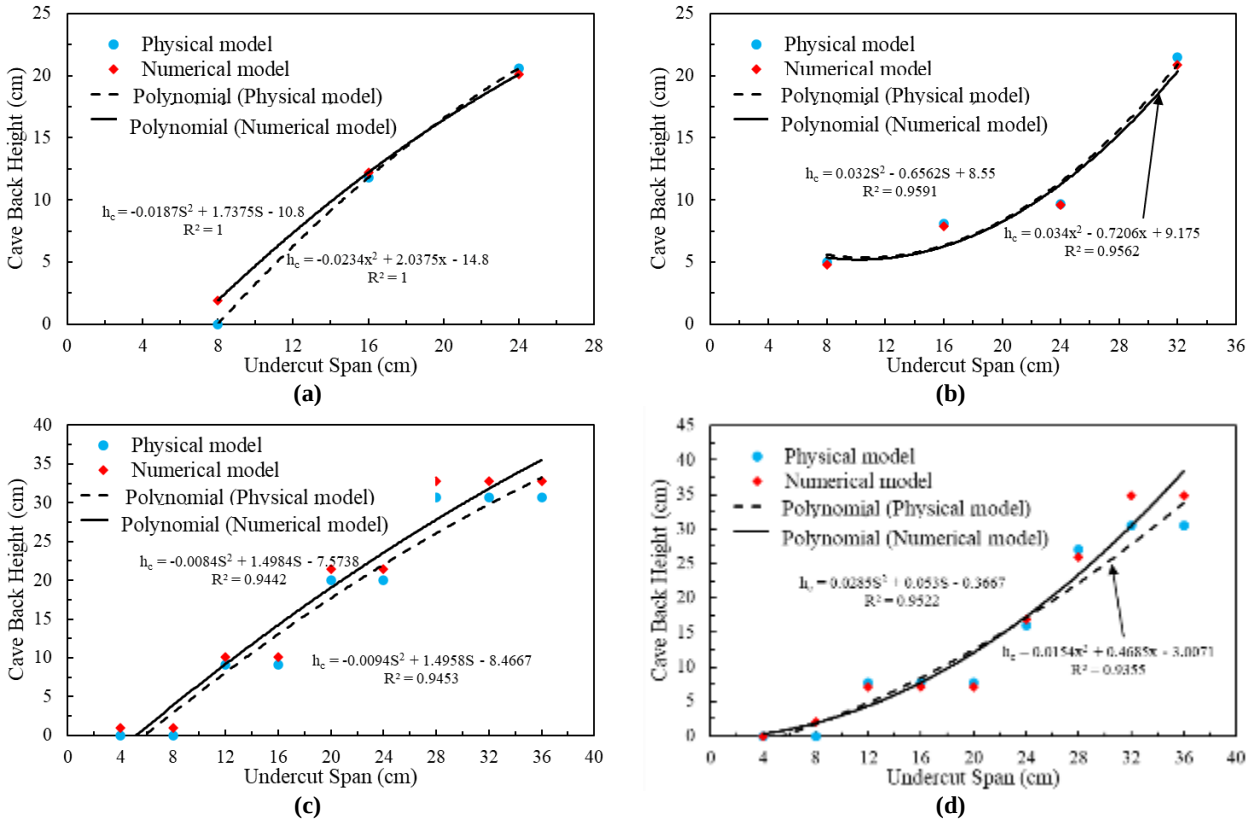

Figure 19. Comparing the results of physical and numerical modeling for the size of an 10cm block: a) 30 and symmetrical undercutting, b) 45 and symmetrical undercutting, c) 60 and advanced undercutting, d) 75 and advanced undercutting.

6. Mathematical modeling

In this section, the authors focused on the mathematical approach. Hence, three mathematical models have been proposed based on the shape of the caving zone in physical models (see Figure 12-15), three mathematical models have been proposed. The models are based on the volume expansion factor, which is similar to that Majdi [28] proposed to estimate the height of the caving zone above the extracted panel roof in longwall coal mining. They assumed different shapes for the caving zone in two dimensions and then calculated the height of the caving zone concerning the height of the extractive coal seam and the volume expansion factor.

6.1. Sub-model 1

In this model, it is assumed that the shape of the caving zone is similar to the parallelogram shown in Figure 20a). Like Majdi et al.'s model, the cross-sectional area of the broken material "α" is assumed to be the cross-sectional area of the caving area. Therefore, the height of the caving zone can be estimated with the following equation:

$$H_c = \frac{h_u}{\alpha} \quad (2)$$

where:

$\boldsymbol{h_u}$**:** undercut height (m)

$\boldsymbol{H_c}$**:** Height of caving zone (m)

6.2. Sub-model 2

In this model, it is assumed that the shape of the caving zone is similar to a trapezoid, as shown in Figure 20b. Identical to the previous model, the height of the caving zone can be estimated as follows:

$$H_c = \frac{-\alpha B + \sqrt{\alpha^2 B^2 + 4A\alpha B H_u}}{2A\alpha} \quad (3)$$

$$A = {}^{1}/_{2\tan(\beta)} \quad (4)$$

where:

B: undercut span (m)

$\boldsymbol{H_c}$: Height of caving zone (m)

$\boldsymbol{\beta}$ **:** dip of joint (degree)

A: is a coefficient obtained from equation 3.

Equation 2 incorporates the span of the undercut and the dip of joints to estimate the height of the caving zone.

6.3. Sub-model 3

In this model, it is assumed that the shape of the caving zone is similar to a trapezoid, as shown in Figure 20c. Identical to the previous model, the height of the caving zone can be estimated with the following equation:

$$H_c = \frac{H_u}{\alpha} + \frac{B.tan(\beta)}{2} \quad (5)$$

Equation 4 incorporates both the span of the undercut and the dip of the joint to estimate the height of the caving zone. It is clear that as the joint dip and the span of undercut increase, the height of the caving zone also increases.

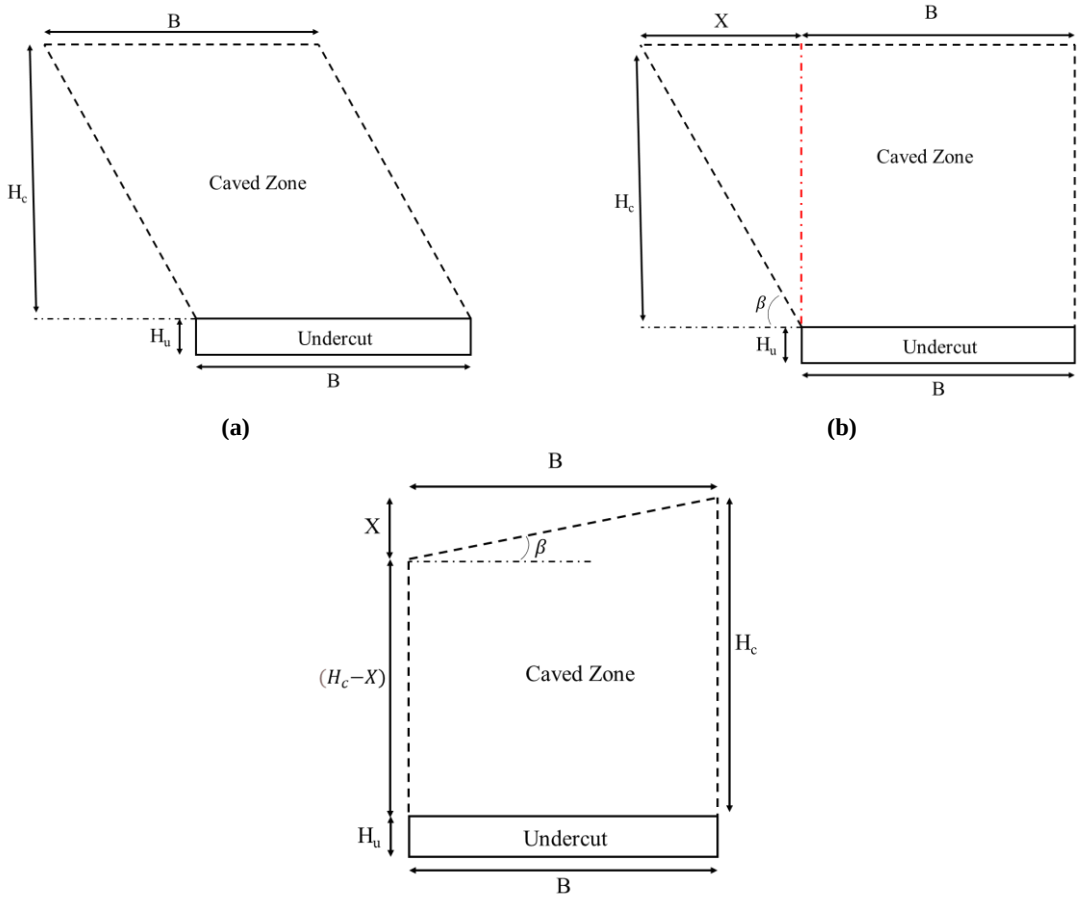

Figure 20. Form of the caving height problem based on the results of the physical model

7. Conclusions

The purpose of this paper was to study the effect of the dip of joint, joint spacing, and undercutting method on the height of the caving zone. Physical modeling and numerical modeling were used for this purpose. A base friction table was used, and the rock mass was simulated using base friction powder. By conducting a series of tests, the appropriate unit weight of the base friction powder was selected for use in the physical model tests by considering two limitations. First, at this unit weight, the blocks made were weak enough to break during tests by applying the force of the base friction table, and second, the blocks made were strong enough to be able to move and place them on the base friction table. The results of the tests showed that the highest caving zone occurs at the angles of 75, followed by the angles of 45, 30 degrees, and 60, respectively. In addition, the cases of 75, 45, and 30 have a relatively positive effect in increasing the height of the caving zone. In comparison, the case of angles of 60 causes a relative decrease in the height of the caving.

The highest caving zone is obtained in blocks with the smallest joint spacing, and the caving height decreases with increased joint spacing. In addition, blocks with a spacing of 4 and 6 cm have a relatively positive effect in increasing the height of caving, while blocks with a spacing of 8 and 10 cm cause a relative decrease in the height of caving. Also, the results showed that the advanced undercutting method causes a relative increase, and the symmetrical undercutting causes a relative decrease in the height of the caving zone. Among the three investigated parameters, the dip of the joint, the method of undercutting, and the spacing of the joints affect the caving height, respectively.

References

[1]. Hartman, H. L., & Mutmansky, J. M. (2002). *Introductory mining engineering*. John Wiley & Sons.

[2]. Brown, E. T. (2002). *Block caving geomechanics*.

[3]. Vakili, A., & Hebblewhite, B. K. (2010). A new cavability assessment criterion for longwall top coal caving. *International Journal of Rock Mechanics and Mining Sciences*, *47*(8).

[4]. Oh, J., Bahaaddini, M., Sharifzadeh, M. and Chen, Z., (2019). Evaluation of air blast parameters in block cave mining using particle flow code. *International Journal of Mining, Reclamation and Environment*, *33*(2), 87–101.

[5]. Guest, A. (2021). Dennis Laubscher, Pioneer of block caving. *Journal of the Southern African Institute of Mining and Metallurgy*, *121*(5).

[6]. Alipenhani, B., Bakhshandeh Amnieh, H., & Majdi, A. (2022a). Application of finite element method for simulation of rock mass caving processes in block caving method. *International Journal of Engineering, Articles in Press*.

[7]. Alipenhani, B., Bakhshandeh Amnieh, H., & Majdi, A. (2022b). Physical model simulation of block caving in jointed rock mass. *International Journal of Mining and Geo-Engineering*.

[8]. Alipenhani, B., Hassan Bakhshandeh Aminieh, & Abbas Majdi. (2023). Investigating mechanical and geometrical effects of joints on minimum caving span in mass caving method. *International Journal of Mining and Geo-Engineering*, *57*(2), 223–229.

[9]. Alipenhani, B., Majdi, A., & Bakhshandeh Amnieh, H. (2022a). Cavability Assessment of Rock Mass in Block Caving Mining Method based on Numerical Simulation and Response Surface Methodology. *Journal of Mining and Environment*, *13*(2), 579–606.

[10]. Rafiee, R., Ataei, M., KhaloKakaie, R., Jalali, S. E., & Sereshki, F. (2016). A fuzzy rock engineering system to assess rock mass cavability in block caving mines. *Neural Computing and Applications*, *27*(7).

[11]. Rafiee, R., Ataei, M., Khalokakaie, R., Jalali, S. M. E., & Sereshki, F. (2015). Determination and assessment of parameters influencing rock mass cavability in block caving mines using the probabilistic rock engineering system. *Rock Mechanics and Rock Engineering*, *48*(3).

[12]. Rafiee, R., Ataei, M., KhalooKakaie, R., Jalali, S. E., Sereshki, F., & Noroozi, M. (2018). Numerical modeling of influence parameters in cavabililty of rock mass in block caving mines. *International Journal of Rock Mechanics and Mining Sciences*, *105*, 22–27.

[13]. Mohammadi, S., Ataei, M., Kakaie, R., Mirzaghorbanali, A., & Aziz, N. (2021). A probabilistic model to determine main caving span by evaluating cavability of immediate roof strata in longwall mining. *Geotechnical and Geological Engineering*, *39*(3).

[14]. Alipenhani, B., Majdi, A., & Bakhshandeh Amnieh, H. (2022b). Determination of Caving Hydraulic Radius of Rock Mass in Block Caving Method using Numerical Modeling and Multivariate Regression. *Journal of Mining and Environment*, *13*(1).

[15]. Khosravi, M.H., Pipatpongsa, T., Takahashi, A. and Takemura, J.,. (2011). Arch action over an excavated pit on a stable scarp investigated by physical model tests. *Soils and Foundations*, *51*(4), 723–735.

[16]. Khosravi, M.H., Takemura, J., Pipatpongsa, T. and Amini, M.,. (2016). In-flight excavation of slopes with potential failure planes. *Journal of Geotechnical and Geoenvironmental Engineering*, *142*(5), 06016001.

[17]. Park, D.-W., & Kicker, D. C. (1985). Physical model study of a longwall mine. *Mining Science and Technology*, *3*(1.

[18]. Whittaker, B. N., & Singh, R. N. (1979). Design and stability of pillars in longwall mining. *Min. Eng.(London);(United Kingdom)*, *139*(214).

[19]. McNearny, R. L., & Abel Jr, J. F. (1993). Large-scale two-dimensional block caving model tests. *International Journal of Rock Mechanics and Mining Sciences & Geomechanics Abstracts*, *30*(2), 93–109.

[20]. Cumming-Potvin, D., Wesseloo, J., Pierce, M. E., Garza-Cruz, T., Bouzeran, L., Jacobsz, S. W., & Kearsley, E. (2018). Numerical simulations of a centrifuge model of caving. *Caving 2018: Proceedings of the Fourth International Symposium on Block and Sublevel Caving*, 191–206.

[21]. Jacobsz, S. W., Kearsley, E. P., Cumming-Potvin, D., & Wesseloo, J. (2018). Modelling cave mining in the geotechnical centrifuge. In *Physical Modelling in Geotechnics* (pp. 809–814). CRC Press.

[22]. Bai, Q., Tu, S., & Wang, F. (2019). Characterizing the top coal cavability with hard stone band (s): Insights from laboratory physical modeling. *Rock Mechanics and Rock Engineering*, *52*(5).

[23]. Heydarnoori, V., Khosravi, M. H., & Bahaaddini, M. (2020). Physical modelling of caving propagation process and damage profile ahead of the cave-back. *Journal of Mining and Environment*, *11*(4).

[24]. Nishida, T., Esaki, T., & Kameda, N. (1988). A development of the base friction technique and its application to subsidence engineering. *Proceedings of the International Symposium on Engineering in Complex Rock Formations*, 386–392.

[25]. Aydan, Ö., & Kawamoto, T. (1992). The stability of slopes and underground openings against flexural toppling and their stabilisation. *Rock Mechanics and Rock Engineering*, *25*(3).

[26]. Amini, M., Majdi, A., & Aydan, Ö. (2009). Stability analysis and the stabilisation of flexural toppling failure. *Rock Mechanics and Rock Engineering*, *42*(5).

[27]. Itasca. (n.d.). *UDEC (Universal Distinct Element Code)* (Version 6) [Computer software].

[28]. Majdi, A., Hassani, F. P., & Nasiri, M. Y. (2012). Prediction of the height of destressed zone above the mined panel roof in longwall coal mining. *International Journal of Coal Geology*, *98*, 62–72.

تعیین ارتفاع منطقه تخریب با استفاده از مدلسازی عددی و فیزیکی بر حسب روش زیربری، شیب و فاصله‌داری درزه

بهنام علی پنهانی[۱]، مهران جلیلیان[۱]، عباس مجدی[۱*]، حسن بخشنده امنیه[۱] و محمدحسین خسروی[۲]

۱. دانشکده مهندسی معدن، دانشگاه تهران، تهران، ایران
۲. گروه مهندسی معدن، دانشگاه بیرجند، بیرجند، ایران

ارسال ۲۰۲۳/۱۲/۲۱، پذیرش ۲۰۲۴/۰۴/۱۲

* نویسنده مسئول مکاتبات: amajdi@ut.ac.ir

چکیده:

در این مقاله تأثیر شیب درزه، فاصله‌داری درزه و روش زیربری بر ارتفاع منطقه تخریب در روش تخریب بزرگ بررسی شده است. نتایج به‌دست‌آمده نشان می‌دهد که از بین سه پارامتر مورد بررسی، به ترتیب شیب درزه، روش زیربری و فاصله‌داری درزه بیشترین تأثیر را بر ارتفاع منطقه تخریب دارند. مقایسه داده‌های به‌دست‌آمده از مدل‌سازی فیزیکی و عددی تطابق ۹۷ درصدی را نشان می‌دهد. در مدل فیزیکی با افزایش فاصله‌داری درزه از ۴ به ۶ سانتی متر، ۱۴ درصد، از ۶ به ۸ سانتی متر، حدود ۳۵ درصد و از ۸ به ۱۰، حدود ۵۰ درصد، ارتفاع منطقه کاهش یافته است. در مورد شیب درزه، با افزایش شیب از ۳۰ به ۴۵ درجه، حدود ۳ درصد از ارتفاع منطقه تخریب کاهش می‌یابد. با افزایش شیب درزه از ۴۵ به ۶۰ درجه، ارتفاع تخریب ۴۲ درصد کاهش یافته است. با افزایش این مقدار از ۶۰ به ۷۵ درجه، ارتفاع تخریب ۵۰ درصد افزایش یافته است. همچنین تغییر روش زیربری از متقارن به زیربری پیشرو باعث افزایش ۴۰ درصدی ارتفاع تخریب می‌شود. علاوه بر این، سه مدل ریاضی بر اساس شکل منطقه تخریب در مدل‌سازی فیزیکی ارائه شده است.

کلمات کلیدی: تخریب بزرگ، مدلسازی فیزیکی، مدلسازی عددی، ارتفاع منطقه تخریب، میز اصطکاک پایه.